ULTRASONIC METHODS FOR DETECTION OF MICRO POROSITY IN COMPOSITE MATERIALS

Jennifer E. Michaels, Thomas E. Michaels and Staffan Jönsson*
Panametrics, Inc.
Automated Systems Division
102 Langmuir Lab
95 Brown Road
Ithaca, NY 14850

*FFV Materialteknik, AB
Linköping, Sweden

INTRODUCTION

Porosity that is detrimental to the performance of a composite structure is often much smaller than can be detected using conventional ultrasonic testing methods. The direct ultrasonic reflection can be too small to detect, and the back wall and through transmission signals may not be significantly changed in amplitude. Thus, improved inspection methods to detect and quantitatively measure micro porosity are of considerable interest. The goals of the study reported here were to (1) evaluate conventional pulse echo and through transmission methods for detection and characterization of micro porosity in composite materials, (2) develop signal processing methods for measuring micro porosity content, and (3) compare results of developed algorithms to conventional inspection results.

DESCRIPTION OF SPECIMENS

Composite panel specimens were prepared with different amounts of micro porosity by varying parameters in the manufacturing process. Sections of each panel were destructively analyzed to determine the actual percentage of porosity and the nature of it. The remainder of each panel was available for ultrasonic testing. Table I summarizes the characteristics of the specimens tested for this study. The porosity content of the tested panels ranged from approximately 0 to 3 percent with a measurement accuracy of up to about 0.8.

Review of Progress in Quantitative Nondestructive Evaluation, Vol. 12
Edited by D.O. Thompson and D.E. Chimenti, Plenum Press, New York, 1993

Table I. Specimen Characteristics

Specimen ID	Thickness (inches)	Porosity Content (%)
1-2.0	0.084	0.80 +/- 0.77
1-3.0	0.084	0.06 +/- 0.21
1-5.0	0.084	0.00 +/- 0.01
1-1.5-5	0.220	2.86 +/- 0.76
1-2.5-5	0.220	0.25 +/- 0.34
1-3.0-5	0.220	0.16 +/- 0.37

CONVENTIONAL ULTRASONIC INSPECTION RESULTS

The samples were first tested using conventional ultrasonic inspection techniques with a Panametrics Multiscan system. Pulse echo and through transmission C-Scan results are shown in Figure 1 for the 0.22 inch thick specimens. A matched pair of 15 MHz broadband transducers were used to generate these images. The pulse echo results are shown as two images: (1) peak amplitude at the approximate center of the specimen, and (2) the amplitude of the back wall echo. The through transmission image is the peak amplitude of the signal transmitted through the specimen.

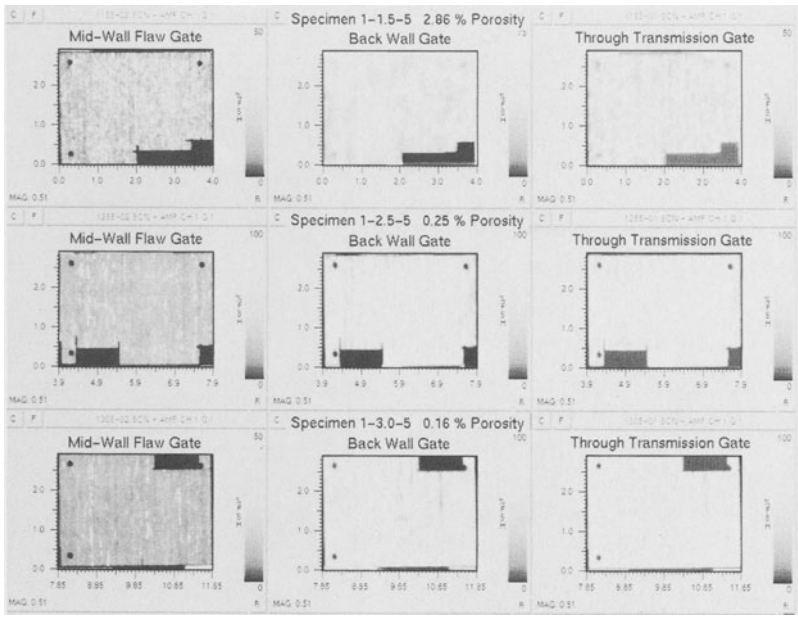

Figure 1. Pulse echo and through transmission images.

The pulse echo response from the back surface echo of the specimens produced essentially the same image as the through transmission results; i.e. both of these images exhibit a decrease in energy at regions of high porosity. We would expect this to be the case, and results here confirm that either method would be suitable for identifying areas of high attenuation in the samples. However, for the pulse echo response from the back wall, the wave path involves two transits through the specimen, whereas there is only one transit for the through transmission wave path. As a result, less detail is evident on the pulse echo image, especially for the higher porosity specimen.

As the porosity increases, both the back wall and through transmission echoes show a progressively larger variation in the amplitude of the signal transmitted through the specimen. Larger amplitude signals appear as light patches on the C-Scan images from Specimen No. 1-1.5-5. The difference in transmitted amplitude between these light areas and the dark areas of the images is approximately 20 dB in signal level. At this time we do not understand why this effect is localized to specific areas, whereas the response from the mid-wall pulse echo flaw gate is fairly uniform across the specimen.

The pulse echo C-Scans from the mid-wall flaw gate show high echo returns from individual porosity sites within the material. Generally, the number of echo sites increases as porosity increases. This is further shown in Figure 2 where signal returns from a horizontal slice near the center of the image are compared. Note that there are only four peaks with a signal return above 50 percent for the 0.16 percent porosity specimen, whereas there are more than twenty for the 2.86 percent porosity specimen. This difference suggests that a peak counting algorithm might be useful for quantitative measurement of porosity in composite materials; however, this approach was not investigated any further in this study.

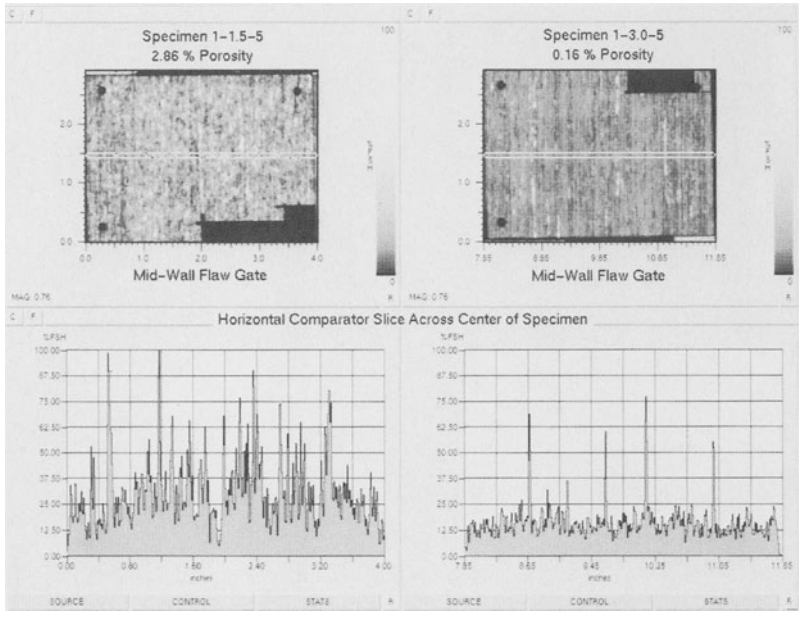

Figure 2. Comparison of mid-wall flaw gate data.

ULTRASONIC ATTENUATION MEASUREMENTS

Measurements were next made of ultrasonic attenuation as a function of frequency by comparing the broadband signal transmitted through specimens to the signal transmitted through a water gap between a matched pair of sending and receiving transducers. These measurements were implemented by collecting a through transmission B-Scan along a line through the center of each of the specimens. The waveforms were digitized at 200 MHz and stored on disk for subsequent analysis.

Measurements were made with several transducers in a frequency range from 5 to 35 MHz. Best results were obtained with a pair of 25 MHz broadband transducers. We experimentally determined that it was best to separate the transducers about 25 percent beyond the distance at which each transducer was focused on the surface of the specimen. This increased separation enlarged the effective "spot size" of the beam and thereby minimized direct blockage of the beam from isolated inclusions. However, it did cause some structure in the frequency spectrum.

One of these line B-Scans is shown in Figure 3 along with the computed frequency spectrum. Again, note the large variation in the overall energy transmitted through this specimen; i.e. there is about a 20 db difference between the "hot" and "cold" spots along this line B-Scan. The structure in the frequency spectrum is seen as dark, vertical bands in the frequency B-Scan.

The ultrasonic attenuation (α) was computed by dividing the reference spectrum by the measured spectrum, taking the natural logarithm, and dividing by the thickness. Thus, the units of attenuation are given in "inches^{-1}". This procedure is illustrated in Figure 4 by showing signals and spectra at different stages of this calculation. The measured waveform is from the line B-Scan of specimen 1-2.5-5.

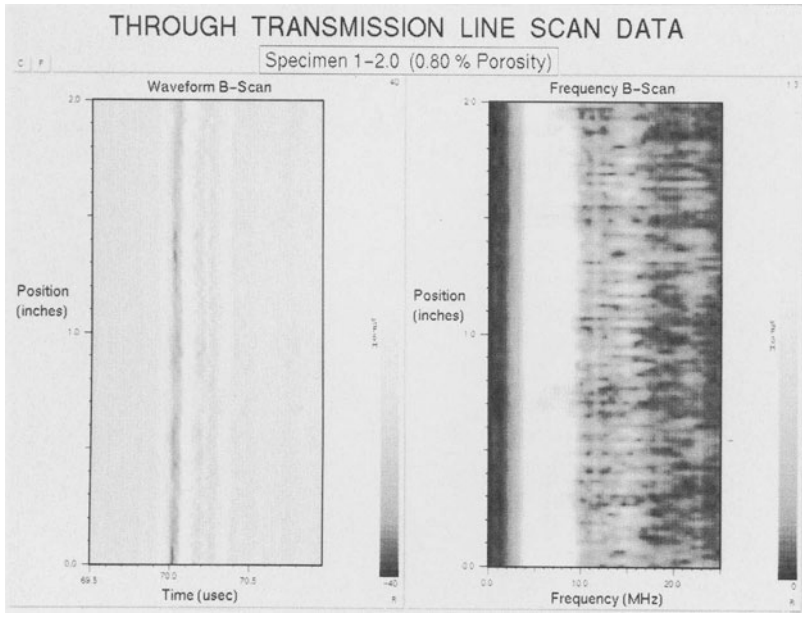

Figure 3. Line waveform and frequency B-Scan images.

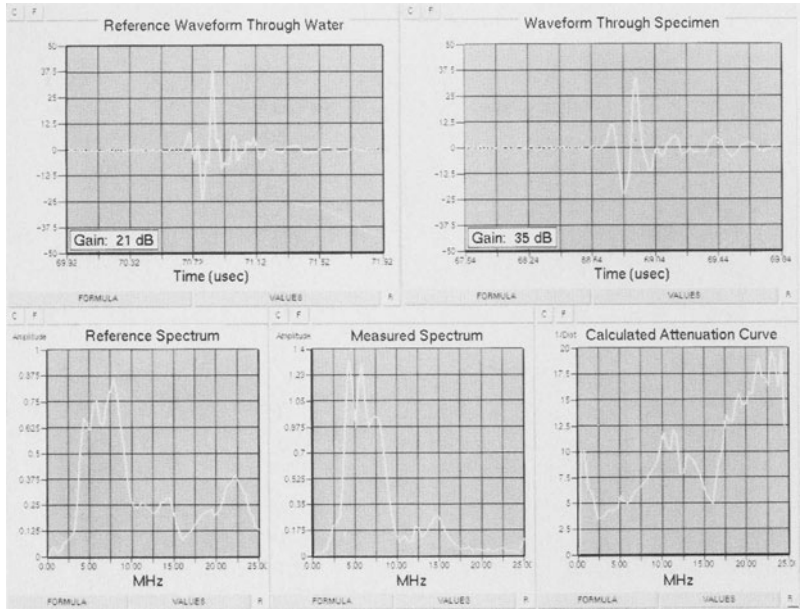

Figure 4. Calculation of attenuation curves.

Note that there is some structure to the frequency spectrum. In particular, there is a minimum near 16 MHz. This structure causes a dip in the attenuation curve which is largely an artifact due to the low energy content in the transmitted energy near this frequency. This structure is part of the compromise in operating slightly out of focus to minimize complete blockage of the transmitted beam by small pores in the specimen. Thus, attenuation results in the range from 12 to 18 MHz are only qualitative. The computed attenuation curves as a function of frequency are show in Figures 5 and 6 for the 0.084 inch and 0.220 inch thick specimens, respectively. For both sets of specimens, the general trend of increasing attenuation with frequency is seen to be a strong function of porosity.

Average attenuation curves for each specimen were calculated by averaging the RF waveforms along each line B-Scan. The resulting attenuation curves are shown in Figure 7. There are several ways to interpret these results, but the usual method is to attempt to correlate the slope of the attenuation vs. frequency (α vs. f) curve to the degree of micro porosity present in the samples. This was done by fitting a straight line to the portion of the curve from 3 to 8 MHz. The resultant intercept and slope values for each specimen are listed in Table II. From these values, it can be seen that there is a good correlation between slope and porosity. A linear curve fit of porosity to slope yields the following relationship:

$$\text{Porosity } (\%) = -0.955 + 1.345 \times \text{Slope } (\alpha \text{ vs. f})$$

This equation provides a means of calculating porosity content directly from attenuation measurements. It should be thought of as an approximate relationship due to the large variations in the porosity measurements for the specimens tested.

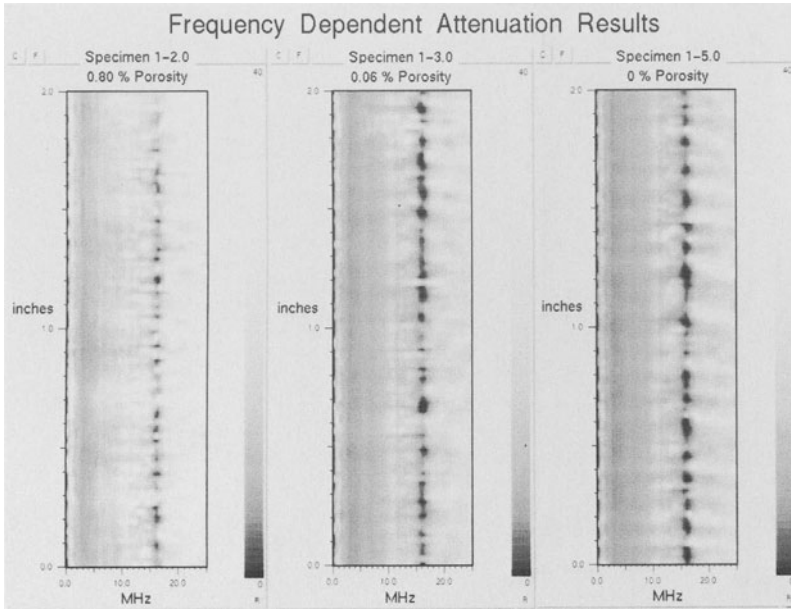

Figure 5. Attenuation images from 0.084 inch thick specimens.

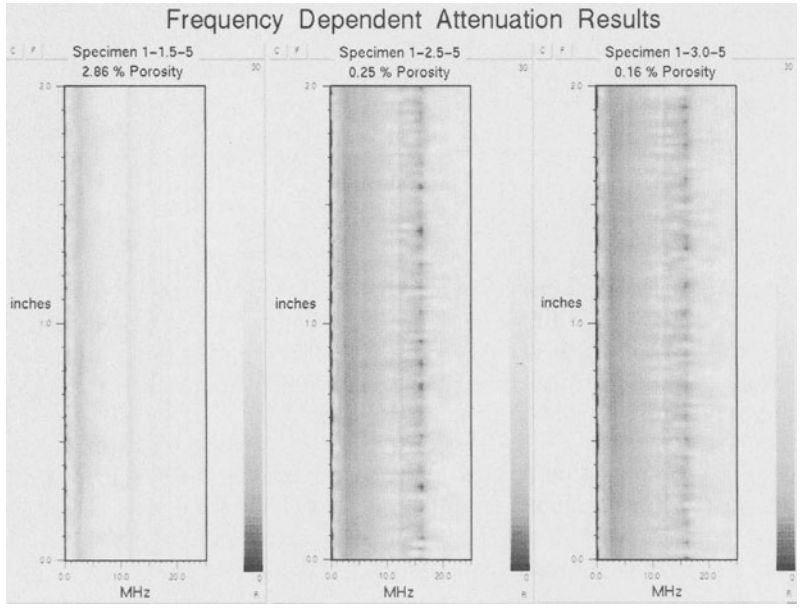

Figure 6. Attenuation images from 0.220 inch thick specimens.

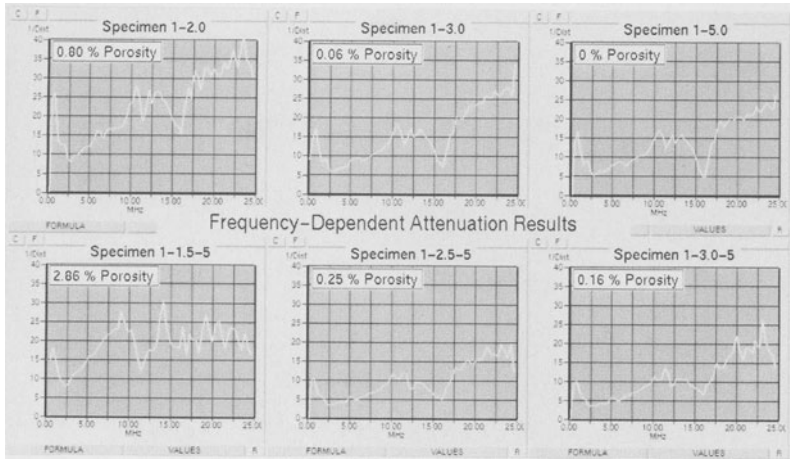

Figure 7. Attenuation curves calculated from spatially averaged waveforms.

Table II. Attenuation Linear Curve Fit Results

Specimen ID	Porosity (%)	Intercept	Slope
1-2.0	0.80	4.34	1.70
1-3.0	0.06	3.35	0.95
1-5.0	0.00	3.64	0.79
1-1.5-5	2.86	2.38	2.59
1-2.5-5	0.25	1.95	0.62
1-3.0-5	0.16	1.77	0.69

SUMMARY AND CONCLUSIONS

Conventional ultrasonic pulse echo and through transmission results showed evidence in C-Scan images of differences in micro porosity. A general increase in discrete reflectors was noted on the pulse echo C-Scan images for a testing frequency of 15 MHz. Although not investigated here, it is thought that the density of such reflectors might serve as a useful index of the amount of porosity.

The through transmission images became progressively more textured with increasing porosity. The variations were irregular with large local areas differing from adjacent areas by as much as 20 db. Because of these variations, it was necessary to develop a technique which averaged measurements over a significant area.

Attenuation curves as a function of frequency were calculated from spatially averaged through transmission waveforms. The slope of the resultant attenuation curve showed a strong correlation to porosity. A linear equation was obtained for computing porosity content from the slope of the ultrasonic attenuation curve.